New far-infrared laser lines and assignments for $^{13}CH_3OH$ methanol

Li-Hong Xu*

Molecular Physics Division, National Institute of Standards and Technology, Gaithersburg, Maryland 20899

R. M. Lees

Department of Physics, University of New Brunswick, Fredericton, New Brunswick, Canada E3B 5A3

E. C. C. Vasconcellos,† L. R. Zink,‡ K. M. Evenson, and S. C. Zerbetto†

Time and Frequency Division, National Institute of Standards and Technology, Boulder, Colorado 80303

Adriana Predoi

Department of Physics, University of New Brunswick, Fredericton, New Brunswick, Canada E3B 5A3

Received March 27, 1995; revised manuscript received July 5, 1995

The $^{13}CH_3OH$ isotopomer of methanol has been reinvestigated as a source of far-infrared (FIR) laser emission by the use of the extended line coverage available from an efficient CO_2 laser recently developed for optical pumping. With this system we have observed 19 new FIR laser lines, pumped by 11 different CO_2 transitions, with five of the pump lines belonging to the new 9*HP* CO_2 hot band. Accurate heterodyne frequency measurements of the FIR laser and the pump offset have been made for 16 FIR laser lines, including three previously reported in the literature. High-resolution Fourier-transform spectroscopic results for the CO-stretching and the CH_3-rocking infrared fundamentals of $^{13}CH_3OH$ have been applied to assign the pump and lasing lines for five of the transition systems. One system has the novel feature that two different CO_2 pump lines excite the same upper level, and hence two FIR laser lines of the identical frequency are observed for two different pump lines.

1. INTRODUCTION

Methanol and its various isotopomers are known as excellent sources of far-infrared (FIR) laser radiation when optically pumped with CO_2 lasers. Since the first discovery of methanol FIR laser emission in 1970,[1] many investigators have searched for new FIR laser lines to meet the needs of experimentalists in such areas as laser magnetic resonance spectroscopy, FIR laser sideband spectroscopy, plasma diagnostics, and a wide variety of solid-state physics studies. These efforts have generated a large catalog of over 2000 discrete methanol FIR laser lines extending from 19.5 to 3030 μm,[2–4] a factor of 155 in wavelength! Nevertheless, there is a continuing need to cover the entire FIR region with as many frequencies as possible; hence the recent development of a high-resolution CO_2 laser that oscillates on many new CO_2 lines[5,6] has an important application in the production of further strong FIR laser emission from methanol.[7] In this paper we present results obtained for the $^{13}CH_3OH$ methanol isotopomer through the enhanced spectral coverage of the modified CO_2 laser. We have found FIR laser lines optically pumped by high-J lines of the regular 9-μm CO_2 laser band as well as by lines of the new 9-μm hot band and the 9-μm sequence band. This experimental detective work has been backed up by detailed spectroscopic studies that have led to assignments for several of the FIR laser transition systems and have revealed the energy-level structure responsible for the laser action. The new laser lines originate from both the excited CO-stretching and the in-plane CH_3-rocking vibrational states of the molecule.

Since FIR laser emission was first reported for $^{13}CH_3OH$ by Henningsen and Petersen in 1978,[8] numerous papers have announced additional FIR laser lines. These are reviewed in Refs. 3 and 4, and transition assignments and associated spectroscopic results are presented in Refs. 9–19. The double-resonance IR experiments of Petersen gave particularly clear identification of certain of the optically pumped transition systems,[10,13] and the extensive IR and FIR Fourier-transform studies carried out by the University of New Brunswick group[12,15,17,18] allowed stringent tests of the proposed assignments and the determination of accurate FIR laser wave numbers by the use of transition combination loops. Most of the earlier reports dealt with pumping in the strong CO-stretching band; however, FIR laser transition systems have also recently been identified for the CH_3 in-plane rocking mode.[19] The center of the weak CH_3-rocking band is close to the 9-μm CO_2 regular and hot bands, giving good possibilities for coincidences between CO_2 lines and rocking-band IR pump absorptions.

In this paper we report the wavelengths for 19 new FIR laser lines of $^{13}CH_3OH$ optically pumped by 11 different CO_2 lines, five of which belong to the new 9*HP* CO_2 hot band.[5] Accurate frequency measurements and pump offsets are presented for 13 of the new FIR laser

0740-3224/95/122352-08$06.00

Table 1. New FIR Laser Lines with Frequency and Offset Measurements for $^{13}CH_3OH$ Optically Pumped by a CO_2 Laser

CO_2 Pump	ν_{CO_2} (cm^{-1})	FIR Laser Line λ (μm)[a]	ν (cm^{-1})[a,b]	ν_{FIR} (MHz)[c]	Offset (MHz)	Rel. Pol.	Pressure (mTorr)	Rel. Int. (mV)	Ref.
9*R*(54)	1096.51636	100.3[d]	99.70				200	0.5	
9*R*(50)	1094.78646	238.43	41.94046	1,257,343.3	−31.4	∥	100	0.25	
		354.32	28.22327	846,112.2	−31.4	∥	100	0.1	
		644.0[d]	15.53		−31.4	⊥	100	0.1	
9*P*(48)	1018.90069	100.57	99.42859	2,980,794.1			300	0.5	4
9*P*(44)	1023.18938	89.13	112.19553	3,363,537.3	−13.8	∥	100	0.15	21
9*P*(42)	1025.29786	116.77	85.63671	2,567,324.1	−16.6	∥	350	0.8	
		125.10	79.93570	2,396,411.9	20.5	∥	300	0.2	
9*P*(4)	1060.57067	168.80	59.24110	1,776,003.4	−7.0	∥	150	0.15	
		189.99	52.63306	1,577,899.4	−47.0	∥	150	0.4	22
9*P*(2)	1062.16597	294.0[d]	34.01				200	0.6	
		208.2[d]	48.03				150		
9*HP*(22)	1052.70174	131.51	76.04178	2,279,675.2	−8.7	∥	100	3.0	
		250.0[d]	40.00			∥	180	14.0	
9*HP*(20)	1054.55242	103.08	97.00941	2,908,268.8	−6.6	∥	150	0.6	
9*HP*(16)	1058.17172	208.27	48.01457	1,439,440.5	−22.1	∥	200	3.0	
9*HP*(12)	1061.68092	292.95	34.13576	1,023,364.2	15.2	∥	100	0.2	
		414.7[d]	24.12				150	weak	
		880.0[d,e]	11.36				110	very weak	
9*HP*(11)	1062.59987	204.44	48.91486	1,466,430.6	−0.8	⊥	100	0.3	
		253.23	39.49038	1,183,891.8	−0.8	∥	100	0.1	
9*SP*(11)	1051.58267	204.44	48.91487	1,466,430.8	36.2	∥	100	0.3	

[a] Calculated from frequency measurement with $c = 2.99792458 \times 10^8$ m/s.
[b] Wave numbers reported to two decimal places are derived from wavelength measurements only.
[c] 1σ uncertainty is $\Delta\nu/\nu = 2 \times 10^{-7}$.
[d] Not frequency measured; wavelength uncertainty is ± 0.5 μm.
[e] Tentative observation.

lines, plus three previously reported lines determined by the heterodyning of the laser output with radiation from two stabilized CO_2 lasers and a microwave synthesizer. Quantum-number identification for the lasing transitions is then made and assignments are given for five of the FIR laser transition systems. These are based on spectroscopic combination relations obtained from our high-resolution IR and FIR Fourier-transform results and comparisons between our calculated spectroscopic wave numbers and the accurate frequency measurements.

2. EXPERIMENTAL ASPECTS

In searching for new IR pump–FIR laser transition systems of $^{13}CH_3OH$, we employed a FIR laser by utilizing a 2-m-long metal-dielectric rectangular waveguide cavity. The cavity is pumped longitudinally through a 1-mm hole in a flat Cu end mirror, described in detail in Ref. 20. The $^{13}CH_3OH$ FIR lasing gas was pumped by a newly developed CO_2 laser that incorporated a 1.5-m ribbed discharge tube and an output coupling taken directly off a specially blazed, 171-line/mm grating. These two features significantly improve the laser mode structure and lead to greatly increased resolution for the line selection.[5,6] Altogether, the CO_2 system lases on more than 200 lines, including the regular 9.4- and 10.4-μm bands from $J = 0$ to $J = 62$, many of the 10.8-μm hot-band lines, many of the 10-μm sequence-band lines, some of the 9-μm sequence lines, and a substantial number of the new 9-μm hot-band lines, with typical power levels of the order of 25 W for the regular lines, 11 W for the hot-band lines, and 6 W for the sequence-band lines.

A. Far-Infrared Laser Wavelength Determination

When new FIR laser lines were sought, the optoacoustic response of the methanol to the chopped CO_2 pumping radiation was first monitored by a microphone placed inside the FIR laser cavity. The CO_2 laser was tuned to maximize the absorption, then the FIR laser cavity length was scanned by the moving of the end mirror connected to a precision micrometer at the far end of the FIR cavity. This micrometer could be continuously driven by a speed-controlled motor for plotting the FIR output. This allowed us to determine the FIR laser wavelengths with an uncertainty of approximately ± 0.5 μm by measuring the distance traveled by the micrometer for 10 or more wavelengths. The FIR laser radiation was coupled out of the cavity by a 45° mirror and detected by a metal–insulator–metal (MIM) diode. The amplitude of the detector signal was recorded as an estimate of the relative intensity of each FIR laser line. A quartz disk was frequently placed in front of the MIM diode in order to block unwanted CO_2 laser radiation. Altogether, we found 19 new FIR laser lines for $^{13}CH_3OH$ with wavelengths of mainly between 100 and 300 μm, pumped by 9-μm regular-, sequence-, and hot-band CO_2 laser lines. Table 1 summarizes the new observations.

B. Heterodyne Far-Infrared Laser Frequency Measurements

For most of the new FIR laser lines, the frequencies were measured to high precision by using the heterodyne technique described in Ref. 23. In this technique, two frequency-stabilized CO_2 lasers, each with an output of a few watts, are locked to the Lamb dips at their respec-

tive line centers. These lasers, of frequencies $\nu_{CO_2}(\mathrm{I})$ and $\nu_{CO_2}(\mathrm{II})$, are mixed on a MIM diode with the unknown FIR laser radiation, ν_{FIR}, plus a microwave signal, $\nu_{\mu\mathrm{wave}}$, supplied in the 2–18-GHz range from a synthesized signal generator. A spectrum analyzer is then employed to search for a beat note from the MIM diode from 0.1 to 1500 MHz. The resulting FIR laser frequency is given by

$$\nu_{\mathrm{FIR}} = |n_1\nu_{CO_2}(\mathrm{I}) - n_2\nu_{CO_2}(\mathrm{II})| \pm m\nu_{\mu\mathrm{wave}} \pm \nu_{\mathrm{beat}}, \quad (1)$$

where n_1, n_2, and m are integers that correspond to the respective harmonics generated in the MIM diode and ν_{beat} is the beat frequency. The intensity of the beat signal decreases as the harmonic orders increase; hence one generally aims to select a suitable pair of CO_2 lines to satisfy the optimum condition $n_1 = n_2 = m = 1$. One determines the appropriate choice of signs in Eq. (1) by noting first whether the beat note increases or decreases as the FIR laser is tuned slightly to a higher frequency and second whether the beat note increases or decreases as the microwave frequency is increased. For the precision measurement of ν_{beat}, the FIR laser is tuned over its gain curve and the signal profile is stored on the spectrum analyzer; then the center of the profile is located by a frequency marker derived from a rf signal generator. In our experiments, three independent measurements of ν_{beat} were generally made for each FIR laser line in order to improve the accuracy and to establish a measure of the scatter. The estimated 1σ relative precision in the reproducibility of the FIR laser frequency measurements is $\Delta\nu/\nu = 2 \times 10^{-7}$.

C. Infrared Pump Offset Measurements

With the rich spectral output available from the efficient, high-resolution CO_2 laser, we found it important to measure the precise IR pump offset for each FIR laser line in order to be absolutely sure of the identity of the CO_2 pump transition. When the latter was located in a dense region of the CO_2 laser spectrum, one could have regular-band, hot-band, and sequence-band laser lines all crowded closely together with significant output powers and not readily distinguishable simply from the setting of the laser-tuning micrometer. We made the offset measurements by adjusting the system to the peak of the FIR emission and then by beating the CO_2 pump laser, ν_{pump}, against a second Lamb-dip-stabilized CO_2 reference laser, ν_{ref}, in a MIM diode. For pumping with the regular CO_2 bands, the reference laser was simply locked to the same line as the main pump laser, and the beat frequency was observed on the spectrum analyzer, giving the pump offset, $|\nu_{\mathrm{pump}} - \nu_{\mathrm{ref}}|$. We readily determined the sign by detuning the CO_2 pump laser slightly to a higher frequency and noting whether the beat note increased or decreased. For sequence- or hot-band pumping, the reference laser was locked to the closest regular-band CO_2 line, and an additional microwave signal, $\nu_{\mu\mathrm{wave}}$, was mixed in to bring the beat note into the range of the spectrum analyzer. The offset was calculated with the relation

$$\nu_{\mathrm{pump}} = (\nu_{\mathrm{ref}} \pm \nu_{\mu\mathrm{wave}}) \pm \nu_{\mathrm{beat}}. \quad (2)$$

Here the correct sign for the microwave sideband was known from the initial choice of a regular CO_2 line to lock at ν_{ref}, while the sign for ν_{beat} was again determined when ν_{pump} was raised slightly and the change of the beat note was noted.

With this heterodyne system, we estimate the uncertainty in the frequency offset measurements to be of the order of ± 2 MHz. The results give accurate center frequencies for the $^{13}CH_3OH$ IR pump absorptions and so serve as an excellent calibration for our Fourier-transform IR (FTIR) spectroscopic wave numbers. The IR pump absorptions for the first three systems of Table 2 are strong and clearly resolved, so they were used to calculate a mean $\nu_{\mathrm{pump}}/\nu_{\mathrm{FTIR}}$ ratio of 1.0000015 from the original FTIR data, which was then used as a calibration factor to obtain the IR wave numbers listed in Table 3.

3. RESULTS

A. Far-Infrared Laser Line Observations

The new data on FIR laser emission from $^{13}CH_3OH$ are listed in Table 1, arranged according to the CO_2 pump lines shown in column 1. The wave numbers of the CO_2

Table 2. Assignments of FIR Laser Lines in $^{13}CH_3OH$ Optically Pumped by a CO_2 Laser

CO_2 Pump + Offset (MHz)	ν_{pump} (cm^{-1})	IR Absorption $P/Q/R(n\tau K, J)^v$	FIR Laser Transition[a] $(n'\tau'K', J')^{v'} \rightarrow (n''\tau''K'', J'')^{v''}$	Line Label	ν_{obs} (cm^{-1})	Rel. Pol.[a]	ν_{calc} (cm^{-1})	Combination Relation
$9R(50) - 31.4$	1094.78541	$R(013^+, 17)^r$	$(013^+, 18)^r \rightarrow (013^+, 17)^r$	L_a	28.22327	$\parallel$	28.2231	$P - m - E$
			$\rightarrow [(022^-, 18)^r]$	$[L_b]$		$[\perp]$	14.1419	$G - (j) + g - (a) - A$
			$\rightarrow (022^+, 17)^r$	L_c	41.94046	$\parallel$	41.9404	$G + d - C$
$9HP(22) - 8.7$	1052.70145	$R(037, 25)^{co}$	$(037, 26)^{co} \rightarrow (037, 25)^{co}$	L_a	40.00	$\parallel$	40.2993	$P + c - f - E$
			$\rightarrow [(016, 26)^{co}]$	$[L_b]$		$[\perp]$	35.7290	$G + a - A$
			$\rightarrow (016, 25)^{co}$	L_c	76.04178	$\parallel$	76.0416	$P + g - D$
$9HP(16) - 22.1$	1058.17098	$R(019, 30)^{co}$	$(019, 31)^{co} \rightarrow (019, 30)^{co}$	L_a	48.01457	$\parallel$	48.0144	$P + (f) - E$
			$\rightarrow [(028, 31)^{co}]$	$[L_b]$		$[\perp]$	63.3770	$P - (e) + b - A$
			$\rightarrow [(028, 30)^{co}]$	$[L_c]$		$[\parallel]$	111.8255	$P + c - C$
$9HP(12) + 15.2$	1061.68143	$Q(025, 9)^r$	$(025, 9)^r \rightarrow [(025, 8)^r]$	$[L_a]$		$[\perp]$	14.1281	$P - F$
			$\rightarrow (034, 9)^r$	L_b	34.13576	$\parallel$	34.1359	$G + c - D$
			$\rightarrow [(034, 8)^r]$	$[L_c]$		$[\perp]$	48.2630	$H + e - C$
$9HP(11) - 0.8$	1062.59984	$Q(026, 6)^r$	$(026, 6)^r \rightarrow (035, 6)^r$	L_b	39.49038	$\parallel$	39.4895	$P_1 + d - B$
			$\rightarrow (035, 5)^r$	L_c	48.91486	$\perp$	48.9147	$P_1 - e + c - C$
$9SP(11) + 36.2$	1051.58388	$P(026, 7)^r$	$(026, 6)^r \rightarrow (035, 5)^r$	L_c	48.91487	$\parallel$	48.9149	$P_2 + c + b - E$

[a]Transitions and polarizations in brackets are predicted.

Table 3. IR and FIR Spectroscopic Wave Numbers[a] for Assigned $^{13}CH_3OH$ IR Pump–FIR Laser Transitions Systems

CO_2 Pump System (MHz)	IR Label	IR Transition	ν_{IR}	FIR Label[b]	FIR Transition	ν_{FIR}[b]
9*R*(50) − 31.4	*P*	$R(013^+, 17)^rA$	1094.78547	(*a*)	$(022^-, 19)^\circ \leftarrow (022^-, 18)^\circ A$	(29.8369)
	A	$P(022^-, 19)^rA$	1031.17191	(*b*)	$(022^-, 18)^\circ \leftarrow (022^-, 17)^\circ A$	(28.2746)
	B	$R(022^-, 17)^rA$	1089.28377	(*c*)	$(022^-, 17)^\circ \leftarrow (022^-, 16)^\circ A$	(26.7110)
	C	$P(022^-, 18)^rA$	1032.88448	*d*	$(013^+, 19)^\circ \leftarrow (022^+, 18)^\circ A$	38.22797
	D	$R(022^-, 16)^rA$	1087.9894*	*e*	$(013^+, 18)^\circ \leftarrow (022^+, 17)^\circ A$	36.6887*
	E	$P(013^+, 18)^rA$	1038.2525*	*f*	$(013^+, 17)^\circ \leftarrow (022^+, 16)^\circ A$	35.14460
	F	$R(013^+, 16)^rA$	1093.3030*	*g*	$(013^-, 19)^\circ \leftarrow (022^-, 18)^\circ A$	38.59287
	G	$P(013^+, 19)^rA$	1036.59694	*h*	$(013^-, 18)^\circ \leftarrow (022^-, 17)^\circ A$	36.97870
				i	$(013^-, 17)^\circ \leftarrow (022^-, 16)^\circ A$	35.37193
				(*j*)	$(013^-, 19)^\circ \leftarrow (013^+, 19)^\circ A$	(0.0391)
				(*k*)	$(013^-, 17)^\circ \leftarrow (013^+, 17)^\circ A$	(0.0205)
				(*l*)	$(013^+, 19)^\circ \leftarrow (013^+, 18)^\circ A$	(29.8783)
				(*m*)	$(013^+, 18)^\circ \leftarrow (013^+, 17)^\circ A$	(28.3098)
				(*n*)	$(013^+, 17)^\circ \leftarrow (013^+, 16)^\circ A$	(26.7405)
9*HP*(22) − 8.7	*P*	$R(037, 25)^{co}A$	1052.70156	*a*	$(037, 27)^\circ \leftarrow (016, 27)^\circ A$	35.58410
	A	$P(016, 27)^{co}A$	969.40129	*b*	$(037, 26)^\circ \leftarrow (016, 26)^\circ A$	35.58945
	B	$R(016, 25)^{co}A$	1052.56738	*c*	$(037, 25)^\circ \leftarrow (016, 25)^\circ A$	35.59503
	C	$P(016, 26)^{co}A$	971.45200	*d*	$(037, 24)^\circ \leftarrow (016, 24)^\circ A$	35.60078
	D	$R(016, 24)^{co}A$	1051.4984*	*e*	$(037, 27)^\circ \leftarrow (016, 26)^\circ A$	77.9470*
	E	$P(037, 26)^{co}A$	971.60392	*f*	$(037, 26)^\circ \leftarrow (016, 25)^\circ A$	76.39322
	F	$R(037, 24)^{co}A$	1051.63956	*g*	$(037, 25)^\circ \leftarrow (016, 24)^\circ A$	74.83846
	G	$P(037, 27)^{co}A$	969.54619			
9*HP*(16) − 22.1	*P*	$R(019, 30)^{co}A$	1058.17072	*a*	$(019, 32)^\circ \leftarrow (028, 31)^\circ A$	117.92488
	A	$R(028, 30)^{co}A$	1062.5999*	*b*	$(019, 31)^\circ \leftarrow (028, 30)^\circ A$	116.38598
	B	$P(028, 31)^{co}A$	965.55590	*c*	$(019, 30)^\circ \leftarrow (028, 29)^\circ A$	114.84475
	C	$R(028, 29)^{co}A$	1061.18997	(*d*)	$(019, 32)^\circ \leftarrow (019, 31)^\circ A$	(50.1340)
	D	$P(019, 31)^{co}A$	961.57592	(*e*)	$(019, 31)^\circ \leftarrow (019, 30)^\circ A$	(48.5798)
	E	$R(019, 29)^{co}A$	1057.18079	(*f*)	$(019, 30)^\circ \leftarrow (019, 29)^\circ A$	(47.0245)
	F	$P(019, 32)^{co}A$	959.4562*			
9*HP*(12) + 15.2	*P*	$Q(025, 9)^rA$	1061.6832*	*a*	$(034, 9)^\circ \leftarrow (034, 8)^\circ A$	14.16635[c]
	A	$R(034, 8)^rA$	1081.87562	*b*	$(034, 8)^\circ \leftarrow (034, 7)^\circ A$	12.59278[c]
	B	$P(034, 9)^rA$	1053.58221	*c*	$(025, 10)^\circ \leftarrow (034, 9)^\circ A$	55.89969
	C	$R(034, 7)^rA$	1080.34131	*d*	$(025, 9)^\circ \leftarrow (034, 8)^\circ A$	54.32864
	D	$Q(034, 9)^rA$	1067.70925	*e*	$(025, 8)^\circ \leftarrow (034, 7)^\circ A$	52.75674
	E	$Q(034, 8)^rA$	1067.74854	*f*	$(025, 10)^\circ \leftarrow (025, 9)^\circ A$	15.73741[c]
	F	$P(025, 9)^rA$	1047.55508	*g*	$(025, 9)^\circ \leftarrow (025, 8)^\circ A$	14.16467[c]
	G	$P(025, 10)^rA$	1045.94539			
	H	$R(025, 8)^rA$	1075.84753			
9*HP*(11) − 0.8	P_1	$Q(026, 6)^rE_2$	1062.5999*	*a*	$(035, 7)^\circ \leftarrow (035, 6)^\circ E_2$	11.01727[c]
9*SP*(11) + 36.2	P_2	$P(026, 7)^rE_2$	1051.58424	*b*	$(035, 6)^\circ \leftarrow (035, 5)^\circ E_2$	9.44377[c]
	A	$P(035, 7)^rE_2$	1057.43942	*c*	$(026, 7)^\circ \leftarrow (035, 6)^\circ E_2$	56.36319
	B	$R(035, 5)^rE_2$	1077.90074	*d*	$(026, 6)^\circ \leftarrow (035, 5)^\circ E_2$	54.7903*
	C	$P(035, 6)^rE_2$	1059.0319*	*e*	$(026, 7)^\circ \leftarrow (026, 6)^\circ E_2$	11.01646[c]
	D	$Q(035, 6)^rE_2$	1068.4569*			
	E	$Q(035, 5)^rE_2$	1068.47631			

[a] Wave numbers (in inverse centimeters) marked with asterisks correspond to overlapped lines and have uncertain accuracy.
[b] Wave numbers for FIR transitions shown in parentheses are calculated by combination differences from CO-stretch IR data.
[c] Converted from the millimeter-wave measurements of Ref. 24 by the use of the factor 1 cm^{-1} = 29,979.2458 MHz.

line centers (ν_{CO_2}) are given in column 2. Columns 3, 4, and 5 list the FIR laser wavelengths in micrometers, the wave numbers in inverse centimeters, and the frequencies in megahertz, respectively, followed in column 6 by the offsets between the pumped IR absorptions and the centers of the CO_2 laser lines, ($\nu_{pump} - \nu_{CO_2}$), expressed in megahertz. The relative polarizations of the CO_2 pump and FIR laser radiation are shown in column 7, the optimum methanol operating pressures for maximum FIR output in column 8, and the approximate relative output intensities of the FIR lines expressed in millivolts of signal on the MIM diode detector in column 9. The final column gives the references for previously observed FIR laser lines[4,21,22] whose frequencies have been measured for the first time in this paper.

A notable feature of interest in Table 1, and a quite unexpected finding, was that the two 9*HP*(11) and 9*SP*(11) CO_2 pump lines independently produce what is obviously the same FIR laser transition at 204.44 μm but with different polarizations. It turns out that these two CO_2 pump lines do indeed excite the same upper lasing level, as is discussed in Subsection 3.B.

B. Far-Infrared Laser Transition Assignments

We have assigned five FIR laser transition systems that involve six different CO_2 pump lines based on our high-resolution FTIR and FIR spectroscopic data. In this paper, we utilized results from analyses of $^{13}CH_3OH$ spectra recorded at a resolution of 0.002 cm^{-1} from 900–1250 cm^{-1} for the IR CO-stretching and CH_3-rocking bands[17,19] and from 15–125 cm^{-1} for the FIR ground-state torsion-rotation band.[18] A sample of the IR spectrum in the vicinity of the $9R(50)$ CO_2 line is shown in Fig. 1, illustrating the coincidence between this CO_2 line and the $R(17)$ member of the $K = 3A^+$ subbranch of the CH_3-rocking band. The specific wave numbers employed in our assignment schemes are listed in Table 3 along with the IR wave numbers calibrated from the pump offset measurements as described in Subsection 2.C and the FIR wave numbers calibrated with water lines that occur naturally in the spectra. The values enclosed in parentheses for ground-state $\Delta K = 0$ a-type and asymmetry doublet transitions in Table 3 are not direct experimental measurements, but are reliably calculated by combination differences from our CO-stretching IR data. Also, two of the systems involve sufficiently low rotational J values that millimeter-wave measurements are available for the a-type transitions.[24]

Our identifications for the IR pump absorptions coincident with the CO_2 lines and for the FIR laser transitions are presented in Table 2, along with the observed FIR laser polarizations and wave numbers. For comparison, we also give sample spectroscopic wave numbers in Table 2 calculated from the data of Table 3 by using the combination difference relations shown in the last column of Table 2. As can be seen, our spectroscopic values are in excellent agreement with the accurate heterodyne frequency measurements, giving strong confirmation of the assignments.

The notation for the energy levels and transitions in Tables 2 and 3 is one in common use in the FIR laser literature; a state is labeled $(n\tau K, J)^v$, where n is the quantum number that specifies the torsional state, and τ is an index with a value of 1, 2, or 3, which gives the torsional C_3 group species by the rule $(\tau + K)\mathrm{mod}3 = +1, 0,$ or -1 for A, E_1, or E_2 symmetries, respectively. The axial rotational quantum number K is the component of the overall rotational angular momentum J projected along the molecular near-symmetry a axis. Finally, the superscript v denotes the vibrational state, and we use $v = o$ for the ground state, $v =$ co for the CO-stretching state, and $v = r$ for the in-plane CH_3-rocking mode.

An example of the structure of the energy level and transition scheme for the optically pumped FIR laser lines is given in Fig. 2 for the $9R(50)$ CO_2 pump. In this relatively complex system, all the levels are split by asymmetry K doubling and the IR transitions appear in the spectrum as close pairs of lines, as seen in Fig. 1 for the $R(013, 17)^r A^{\pm}$ doublet. The FIR laser lines for this system and others often occur in triads,[25,26] which comprise a $\Delta K = 0$, $\Delta J = -1$ a-type transition (L_a), a $\Delta J = 0$, $\Delta K = -1$ b-type Q-branch transition (L_b), and a $\Delta J = -1$, $\Delta K = -1$ b-type transition (L_c). Because the a-type transition wave numbers depend only weakly on the $(n\tau K)$ quantum numbers, one has the triad rule that $L_a \approx L_c - L_b$. The relative polarizations of the FIR laser lines also have a characteristic fingerprint for a triad. If the transitions for the IR pump and the FIR laser both involve similar changes in J, with $|\Delta J_{\mathrm{FIR}}| = |\Delta J_{\mathrm{pump}}|$, then the FIR laser polarization will be parallel to that of the pump; otherwise, it will be perpendicular.[26,27] Thus one member of the triad will always be polarized differently from the other two. In our investigation, two of the pump lines excite the same lowest $J = K$ level of the stack, so that the L_a transition does not occur. For other systems, few lines with perpendicular polarization were seen, and it is likely in retrospect that the configuration of the FIR laser cavity and antenna pattern of the MIM diode detector favored the parallel lines. However, the perpendicular wave numbers are determined by spectroscopic combination differences to within an uncertainty of approximately ± 0.001 cm^{-1} from the data in Table 3. Therefore these transitions are included in brackets in Table 2 together with their calculated wave numbers for reference and potential future observation.

Of the five assigned transition systems in Table 2, three involve pumping into the CH_3-rocking mode and two into the CO stretch, with one of the latter potentially involving hybridized CO-stretch–CH_3-rock levels. The duplicate 204.44-μm FIR laser lines of Table 1 are indeed assigned to a common transition, because of the remarkable coincidence that both the $9HP(11)$ and the $9SP(11)$ CO_2 lines have access to the same $(026, 6)^r E_2$ excited CH_3-rocking level. The energy level and transition diagram is shown in Fig. 3, and, to our knowledge, this is the first case in which two different CO_2 laser lines optically pump a common upper state. Because the IR absorption is a Q-branch transition for the $9HP(11)$ pump and a P-branch transition for the $9SP(11)$ pump, the FIR laser lines have different polarizations in the two cases, although their frequencies are of course identical. This system is also an exception to the usual triad situation, because the $J = 6$ upper lasing level is the bottom one of the $(026, J)^r$ stack so that no a-type line L_a exists to form the triad.

It is noteworthy that the accurate FIR laser frequency measurements were crucial to the success of the assignment for the $9HP(11)$ system, because the $Q(026, 6)^r$ P_1 pump absorption lies in a broad, blended feature in the spectrum overlapped by both the $R(033, 35)^{co}$ and the $R(028, 30)^{co}$ CO-stretching transitions, and the identity

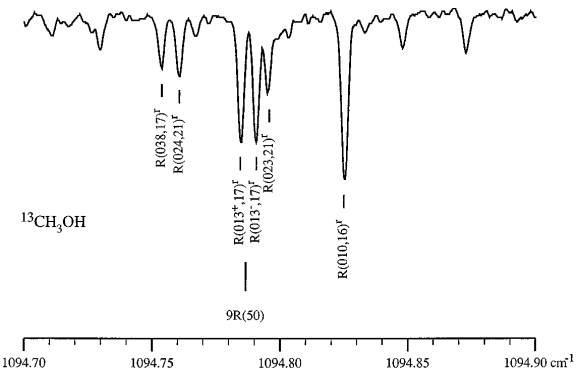

Fig. 1. Part of the Fourier-transform spectrum of $^{13}CH_3OH$ recorded at a resolution of 0.002 cm^{-1}, showing the coincidence between the $9R(50)$ CO_2 line and the $R(013^+, 17)^r A^+$ transition of the in-plane CH_3-rocking band.

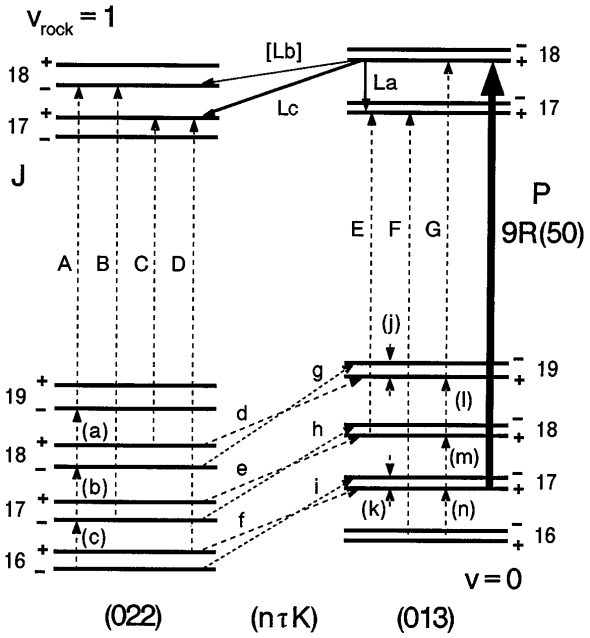

Fig. 2. Energy level and transition scheme for the FIR laser lines of $^{13}CH_3OH$ optically pumped by the 9*R*(50) CO_2 laser line. Line $[L_b]$ is predicted, and the FIR ground-state transitions shown in parentheses have been calculated from IR CO-stretching spectroscopic data by combination differences. Transition wave numbers are given in Table 3.

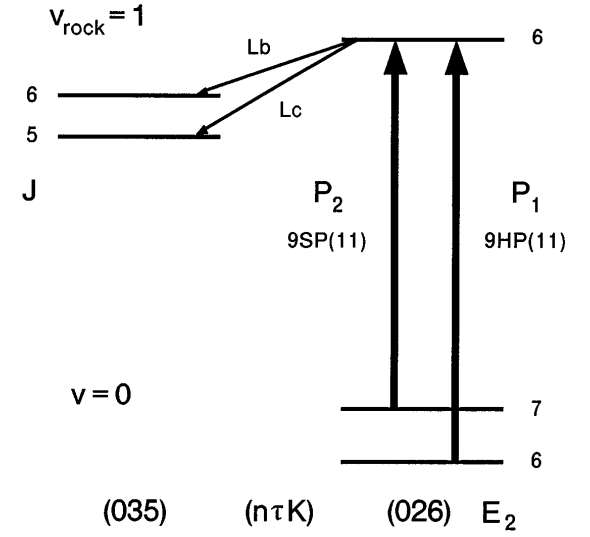

Fig. 3. Energy level and transition scheme for the FIR laser emission of $^{13}CH_3OH$ generated by the 9*HP*(11) hot-band and 9*SP*(11) sequence-band CO_2 lines, in which the same FIR laser transition is optically pumped by two independent CO_2 laser lines.

of the pumped transition was not clear. The frequency measurement was also essential for the confident assignment of the 9*HP*(16) system, for which just a single *a*-type laser line has so far been seen. The *a*-type wave numbers are relatively insensitive to the $(n\tau K)$ quantum state; hence it is normally not possible with the limited accuracy of a wavelength measurement to determine an assignment from a single *a*-type observation.

For the 9*R*(50) system in Fig. 2, two members of the FIR laser triad have been observed and accurately frequency measured. Figure 2 shows a number of IR and FIR transitions that can be used to form closed combination loops for rigorous tests of the assignment scheme, and Table 3 includes the wave numbers for those transitions. For a closed loop of transitions, the sum of the wave numbers around the loop should equal 0 to within a closure defect δ of approximately $\pm 0.001\ cm^{-1}$, representing the net spectroscopic measurement uncertainty for the four transitions. A wide variety of such loops can be formed from the transitions in Fig. 2 to test the assignments for the 9*R*(50) system. A sample of the closure defects and loop relations is given below, as determined from the FIR laser frequency measurements in Table 1 and the spectroscopic data in Table 3:

$$\delta_1 = P + (n) - F - L_a = 1094.7855 + (26.7405) - 1093.3030 - 28.2233 = -0.0003,$$

$$\delta_2 = G + (l) - E - L_a = 1036.5969 + (29.8783) - 1038.2525 - 28.2233 = -0.0006,$$

$$\delta_3 = P + f - D - L_c = 1094.7855 + 35.1446 - 1087.9894 - 41.9405 = 0.0002,$$

$$\delta_4 = G + d - C - L_c = 1036.5969 + 38.2280 - 1032.8845 - 41.9405 = -0.0001.$$

The loop defects are effectively 0 to well within the allowed $\pm 0.001\ cm^{-1}$ tolerance, giving strong support for the spectroscopy and the FIR laser assignments. The wave number for the missing third member of the triad can be calculated from the following loop combination difference relations:

$$[L_b] = P - (k) + i - (c) - B = 1094.7855 - (0.0205) + 35.3719 - (26.7110) - 1089.2838 = 14.1421$$

$$= G - (j) + g - (a) - A = 1036.5969 - (0.0391) + 38.5929 - (29.8369) - 1031.1719 = 14.1419.$$

Again, the good agreement between the $[L_b]$ wave numbers predicted from independent loops is excellent confirmation of the internal self-consistency of the assignments. Note that the triad rule is not closely obeyed for this particular system because of the substantial asymmetry splitting of the $K = 2$ levels.

A system of special spectroscopic significance is that pumped by the 9*HP*(16) CO_2 line. Here, the $(028, 31)^{co}$ and the $(028, 30)^{co}$ CO-stretching levels that could be reached by FIR emission from the pumped $(019, 31)^{co}$ state are known to interact strongly with $(037)^r$ CH_3-rocking levels lying below,[17] and this Coriolis resonance perturbs the excited $(028)^{co}$ CO-stretching levels upward by several inverse centimeters. The $(028)^{co}$ subband behaves quite differently from its fellows in the spectrum, as shown by the fact noted above that the two other IR absorptions overlapping with the $Q(026, 6)^r$ pump line for the 9*HP*(11) system are the $R(028, 30)^{co}$ and the $R(033, 35)^{co}$ transitions. The *J* values for these lines are quite different, demonstrating the substantial shift in the $(028)^{co}$ levels. This can also be seen in Table 3 from the difference between the $R(028, 30)^{co}$ wave number of $1062.59992\ cm^{-1}$ and the more typical $R(019, 30)^{co}$ wave

number of 1058.17072 cm^{-1}. The interaction mixes the $(028)^{co}$ and $(037)^{r}$ levels, so that we might expect potential FIR laser lines between the optically pumped $(019, 31)^{co}$ level and the hybridized $J = 31$ and $J = 30$ CO-stretch–CH_3-rock levels. However, the experimental FIR laser plot for the 208.27-μm line in the 9*HP*(16) system was very clean, and no traces of other lines were visible. Still, it would be useful to check this system carefully again for additional FIR laser lines at the predicted frequencies, as definitive confirmation of the proposed Coriolis mixing and interaction scheme would be valuable spectroscopically. Alternatively, it would be interesting to reexamine the 9*HP*(11) CO_2 system again to attempt to pump directly into the $(028)^{co}$ stack of levels through the $R(028, 30)^{co}$ transition, which must lie very close to the 9*HP*(11) line.

4. DISCUSSION AND CONCLUSIONS

In this paper the extended spectral coverage available from our improved CO_2 laser has been exploited to generate new FIR laser emissions from the $^{13}CH_3OH$ isotopomer of methanol, and 19 new FIR laser lines have been observed. We have measured accurate frequencies and IR pump offsets for 16 FIR laser lines by heterodyning them with frequency radiation generated from stabilized CO_2 lasers and a microwave synthesizer. Assignments have been determined for five of the new IR pump–FIR laser transition systems, three of which are found to involve pumping into the excited in-plane CH_3-rocking mode and two into the CO-stretching mode. A novel and unique feature for one system is that two different CO_2 laser lines pump into the same excited-state level and produce FIR laser lines of identical frequency, the first time this has been observed. Another system involves Coriolis coupling and potential FIR laser emission to postulated hybridized CO-stretch–CH_3-rock doublets; this is of considerable spectroscopic interest.

The FIR laser system assignments are supported by combination loops formed from the IR pump transitions, the FIR laser lines, and IR and FIR transitions derived from spectroscopic studies of the FIR ground-state torsion-rotation band and the IR CO-stretching and CH_3-rocking fundamental bands. The combination loops serve both to confirm the spectroscopic assignments, particularly valuable for the weak CH_3-rocking spectra, and to yield calculated wave numbers for the FIR laser lines with an uncertainty of the order of ± 0.001 cm^{-1}. The loop-calculated wave numbers agree with the heterodyne measurements in all cases. If only the wavelength, but not the frequency, of an FIR laser line is measured, the loop wave number gives a substantial improvement in the accuracy of the transition. Moreover, the combination loops allow prediction of further potential FIR laser lines that have not yet been observed, and the wave numbers for a number of such transitions have been tabulated.

ACKNOWLEDGMENTS

We are pleased to acknowledge financial support for this research from the Division of Chemical Sciences, Office of Basic Energy Sciences, Office of Energy Research, U.S. Department of Energy; the Natural Sciences and Engineering Research Council of Canada and the University of New Brunswick Research Fund; NASA grant W-18, 623; and the Conselho Nacional de Pesquisas of the Brazilian Government. We thank Mario Noel and J. W. C. Johns of the National Research Council of Canada for assistance in obtaining the Fourier-transform spectra.

*National Institute of Standards and Technology Guest Researcher 1994–1995. Permanent address, Department of Physical Sciences, University of New Brunswick, Saint John, New Brunswick, Canada E2L 4L5.
†Permanent address, Departamento de Electronica Quantica, Instituto de Fisica "Gleb Wataghin," Universidade Estadual de Campinas, 13083-970 Campinas, Sao Paulo, Brasil.
‡Permanent affiliation, Cooperative Institute for Research in Environmental Science, University of Colorado and National Oceanographic and Atmospheric Administration.

REFERENCES

1. T. Y. Chang, T. J. Bridges, and E. G. Burkhardt, "cw Submillimeter laser action in optically pumped methyl fluoride, methyl alcohol, and vinyl chloride gases," Appl. Phys. Lett. **17,** 249–251 (1970).
2. G. Moruzzi, J. C. S. Moraes, and F. Strumia, "Far infrared laser lines and assignments of CH_3OH: a review," Int. J. Infrared Millimeter Waves **13,** 1269–1312 (1992).
3. D. Pereira, J. C. S. Moraes, E. M. Telles, A. Scalabrin, F. Strumia, A. Moretti, G. Carelli, and C. A. Massa, "A review of optically pumped far-infrared laser lines from methanol isotopes," Int. J. Infrared Millimeter Waves **15,** 1–44 (1994).
4. S. C. Zerbetto and E. C. C. Vasconcellos, "Far infrared laser lines produced by methanol and its isotopic species: a review," Int. J. Infrared Millimeter Waves **15,** 889–933 (1994).
5. K. M. Evenson, C.-C. Chou, B. W. Bach, and K. G. Bach, "New cw CO_2 laser lines: the 9 μm hot band," IEEE J. Quantum Electron. **30,** 1187–1188 (1994).
6. A. G. Maki, C. -C. Chou, K. M. Evenson, L. Zink, and J. -T. Shy, "Improved molecular constants and frequencies for the CO_2 laser from new high-J regular and hot band frequency measurements," J. Mol. Spectrosc. **167,** 221–224 (1994).
7. L.-H. Xu, R. M. Lees, K. M. Evenson, C.-C. Shou, J.-T. Shy, and E. C. C. Vasconcellos, "Spectroscopy of new CH_3OH FIR laser lines pumped by new CO_2 laser lines," Can. J. Phys. **72,** 1155–1164 (1994).
8. J. O. Henningsen and J. C. Petersen, "Observation and assignment of far-infrared laser lines from optically pumped $^{13}CH_3OH$," Infrared Phys. **18,** 475–479 (1978).
9. R. M. Lees, "Far-infrared and infrared spectroscopy of methanol applied to FIR laser assignments," in *Far-Infrared Science and Technology,* J. R. Izatt, ed., Proc. Soc. Photo-Opt. Instrum. Eng. **666,** 158–170 (1986).
10. J. C. Petersen, "Infrared radio-frequency double resonance of $^{13}CH_3OH$," Opt. Lett. **12,** 471–473 (1987).
11. I. Mukhopadhyay, R. M. Lees, W. Lewis-Bevan, J. W. C. Johns, F. Strumia, and G. Moruzzi, "Applications of high resolution spectroscopy to the identification of far-infrared laser emission from optically pumped $^{13}CH_3OH$," Int. J. Infrared Millimeter Waves **8,** 1483–1502 (1987).
12. I. Mukhopadhyay, R. M. Lees, and J. W. C. Johns, "High-resolution far-infrared spectroscopy of C-13 methanol," Int. J. Infrared Millimeter Waves **9,** 1119–1140 (1988).
13. J. C. Petersen, "Infrared-infrared double-resonance spectra of $^{13}CH_3OH$ and $^{12}CH_3OH$," J. Opt. Soc. Am. B **6,** 350–355 (1989).
14. E. M. Telles, J. C. S. Moraes, A. Scalabrin, D. Pereira, A. Moretti, and F. Strumia, "Doppler-free optoacoustic measurements in FIR laser active molecules," Infrared Phys. **31,** 415–423 (1991).

15. I. Mukhopadhyay and R. M. Lees, "High-resolution spectroscopy of methanol: Coriolis resonances and far infrared laser identification," Opt. Commun. **97,** 194–198 (1993).
16. D. Pereira, F. C. Cruz, J. C. S. Moraes, and A. Scalabrin, "Diode laser and Fourier transform spectroscopy of the $^{13}CH_3OH$ C-O stretching mode," Int. J. Infrared Millimeter Waves **15,** 417–428 (1994).
17. I. Mukhopadhyay, R. M. Lees, W. Lewis-Bevan, and J. W. C. Johns, "Fourier transform spectroscopy of the CO-stretching band of C-13 methanol in the torsional ground state," J. Chem. Phys. **102,** 6444–6455 (1955).
18. I. Mukhopadhyay and R. M. Lees, "Far-infrared spectrum of excited torsional states of C-13 methanol," Int. J. Infrared Millimeter Waves **16,** 99–115 (1995).
19. R. M. Lees, A. Predoi, and L.-H. Xu, "Far infrared laser assignments for CO-stretching and CH_3-rocking states of optically pumped $^{13}CH_3OH$," presented at the Fourth Conference on Optics, ROMOPTO'94, Bucharest, Romania, September, 1994.
20. M. Inguscio, F. Strumia, K. M. Evenson, D. A. Jennings, A. Scalabrin, and S. R. Stein, "Far infrared CH_3F Stark laser," Opt. Lett. **4,** 9–11 (1979).
21. N. Ioli, A. Moretti, F. Strumia, and F. D'Amato, "$^{13}CH_3OH$ and $^{13}CD_3OH$ optically pumped FIR laser: new large offset emission and optoacoustic spectroscopy," Int. J. Infrared Millimeter Waves **7,** 459–486(1986).
22. D. Pereira and A. Scalabrin, "Measurement and assignment of new FIR laser lines in $^{12}CH_3OH$ and $^{13}CH_3OH$," Appl. Phys. B **44,** 67–69 (1987).
23. F. R. Petersen, K. M. Evenson, D. A. Jennings, J. S. Wells, K. Goto, and J. J. Jimenez, "Far infrared frequency synthesis with stabilized CO_2 lasers: accurate measurements of the water vapor and methyl alcohol laser frequencies," IEEE J. Quantum Electron. **QE-11** 838–843 (1975).
24. T. Anderson, E. Herbst, and F. C. De Lucia, "The millimeter- and submillimeter-wave spectrum of $^{13}CH_3OH$ revisited," Astrophys. J. Suppl. **74,** 647–664 (1990).
25. J. O. Henningsen, "New FIR laser lines from optically pumped CH_3OH: measurements and assignments," IEEE J. Quantum Electron. **QE-14,** 958–962 (1978).
26. J. O. Henningsen, "Molecular spectroscopy by far-infrared laser emission," in *Infrared and Millimeter Waves 5. Coherent Sources and Applications,* K. J. Button, ed. (Academic, New York, 1982), Chap. 2, pp. 29–128.
27. J. O. Henningsen, "Assignment of laser lines in optically pumped CH_3OH," IEEE J. Quantum Electron. **QE-13,** 435–441 (1977).